PHYSICAL REVIEW D **76,** 094028 (2007)

Line shapes of the $X(3872)$

Eric Braaten and Meng Lu

Physics Department, Ohio State University, Columbus, Ohio 43210, USA

(Received 18 September 2007; published 28 November 2007)

If the quantum numbers of the $X(3872)$ are $J^{PC} = 1^{++}$, the measurement of its mass implies that it is either a loosely bound hadronic molecule whose constituents are a superposition of the charm mesons pairs $D^{*0}\bar{D}^0$ and $D^0\bar{D}^{*0}$ or else it is a virtual state of these charm mesons. Its binding energy is small enough that the decay width of a constituent D^{*0} or $\bar{D}^{*0}$ has a significant effect on the line shapes of the X resonance. We develop a simple approximation to the line shapes that takes into account the effect of the D^{*0} width as well as inelastic scattering channels of the charm mesons. We carry out a simultaneous fit to the line shapes in the $J/\psi\pi^+\pi^-$ and $D^0\bar{D}^0\pi^0$ channels measured in the decays $B^+ \to K^+ + X$ by the Belle Collaboration. The best fit corresponds to the $X(3872)$ being a bound state just below the $D^{*0}\bar{D}^0$ threshold, but a virtual state just above the $D^{*0}\bar{D}^0$ threshold is not excluded.

DOI: 10.1103/PhysRevD.76.094028 PACS numbers: 12.38.−t, 12.39.St, 13.20.Gd, 14.40.Gx

I. INTRODUCTION

The $X(3872)$ is a hadronic resonance near 3872 MeV discovered in 2003 by the Belle Collaboration [1] and subsequently confirmed by the CDF, *BABAR*, and D0 Collaborations [2–4]. In addition to the discovery decay mode $J/\psi\pi^+\pi^-$, the X has been observed to decay into $J/\psi\gamma$ and $J/\psi\pi^+\pi^-\pi^0$ [5]. The decay into $J/\psi\gamma$ implies that the X is even under charge conjugation. An analysis by the Belle Collaboration of the decays of X into $J/\psi\pi^+\pi^-$ strongly favors the quantum numbers $J^{PC} = 1^{++}$, but does not exclude 2^{++} [6]. An analysis by the CDF Collaboration of the decays of X into $J/\psi\pi^+\pi^-$ is compatible with the Belle constraints [7]. The Belle Collaboration has also discovered a near-threshold enhancement in the $D^0\bar{D}^0\pi^0$ system near 3875 MeV [8]. If this enhancement is associated with the $X(3872)$, the tiny phase space available would rule out $J = 2$, leaving 1^{++} as the only option.

An important feature of the $X(3872)$ is that its mass is extremely close to the $D^{*0}\bar{D}^0$ threshold. The PDG value for M_X comes from combining measurements of X in the $J/\psi\pi^+\pi^-$ decay mode [9]. After taking into account a recent precision measurement of the D^0 mass by the CLEO Collaboration [10], the difference between the PDG value for M_X and the $D^{*0}\bar{D}^0$ threshold is

$$M_X - (M_{*0} + M_0) = -0.6 \pm 0.6 \text{ MeV}, \qquad (1)$$

where M_{*0} and M_0 are the masses of D^{*0} and D^0. The negative central value is compatible with the X being a bound state of the charm mesons. The PDG value for the mass of $X(3872)$ comes from combining measurements of X in the $J/\psi\pi^+\pi^-$ decay mode [9]. The peak of the near-threshold enhancement in $D^0\bar{D}^0\pi^0$ [8] is at a mass satisfying

$$M - (M_{*0} + M_0) = +4.1 \pm 0.7^{+0.3}_{-1.6} \text{ MeV}. \qquad (2)$$

We have obtained this result from the value of M quoted in Ref. [8] by subtracting $2M_0 + (M_{*0} - M_0)$, where M_0 is the 2006 PDG fitted mass for the D^0, and by dropping the error bar associated with the D^0 mass. The positive central value in Eq. (2) is compatible with X being a virtual state of charm mesons. The difference between the masses in Eqs. (1) and (2) is $4.7^{+1.0}_{-1.8}$ MeV. This is more than 2 standard deviations, which raises the question of whether the decays into $J/\psi\pi^+\pi^-$ and $D^0\bar{D}^0\pi^0$ are coming from the same resonance.

The proximity of the mass of the $X(3872)$ to the $D^{*0}\bar{D}^0$ threshold has motivated its identification as a weakly bound molecule whose constituents are a superposition of the charm meson pairs $D^{*0}\bar{D}^0$ and $D^0\bar{D}^{*0}$ [11–14]. The establishment of the quantum numbers of the $X(3872)$ as 1^{++} would make this conclusion almost unavoidable. The reason is that these quantum numbers allow S-wave couplings of the X to $D^{*0}\bar{D}^0$ and $D^0\bar{D}^{*0}$. Nonrelativistic quantum mechanics implies that a resonance in an S-wave channel near a 2-particle threshold has special universal features [15]. Because of the small energy gap between the resonance and the 2-particle threshold, there is a strong coupling between the resonance and the two particles. This strong coupling generates dynamically a large length scale that can be identified with the absolute value of the S-wave scattering length a of the two particles. Independent of the original mechanism for the resonance, the strong coupling transforms the resonance into a bound state just below the 2-particle threshold if $a > 0$ or into a virtual state just above the 2-particle threshold if $a < 0$. If $a > 0$, the bound state has a molecular structure, with the particles having a large mean separation of order a.

The universality of few-body systems with a large scattering length has many applications in atomic, nuclear, and particle physics [16]. To see that these universal features are relevant to the $X(3872)$, we need only note that its binding energy is small compared to the natural energy scale associated with pion exchange: $m_\pi^2/(2M_{*00}) \approx 10$ MeV, where M_{*00} is the reduced mass of the two constituents. The universal features of the $X(3872)$ were first exploited by Voloshin to describe its decays into $D^0\bar{D}^0\pi^0$ and $D^0\bar{D}^0\gamma$, which can proceed through decay

of the constituent D^{*0} or $\bar{D}^{*0}$ [14]. Universality has also been applied to the production process $B \to KX$ [17,18], to the line shapes of the X [19], and to decays of X into J/ψ and pions [20]. These applications rely on factorization formulas that separate the length scale a from all the shorter distance scales of QCD [19]. The factorization formulas can be derived using the operator product expansion for a low-energy effective field theory [21].

Other interpretations of the $X(3872)$ besides a charm meson molecule or a charm meson virtual state have been proposed, including a P-wave charmonium state or a tetraquark state. (For a review, see Ref. [22].) The discrepancy between the masses M_X and M in Eqs. (1) and (2) has been interpreted as evidence that the $J/\psi\pi^+\pi^-$ events and the $D^0\bar{D}^0\pi^0$ events arise from decays of two distinct tetraquark states whose masses differ by about 5 MeV [23]. If the charmonium or tetraquark models were extended to include the coupling of the X to $D^{*0}\bar{D}^0$ and $D^0\bar{D}^{*0}$ scattering states, quantum mechanics implies that the tuning of the binding energy to the threshold region would transform the state into a charm meson molecule or a virtual state of charm mesons. Any model of the $X(3872)$ that does not take into account its strong coupling to charm meson scattering states should not be taken seriously.

We will assume in the remainder of this paper that the quantum numbers of the $X(3872)$ are 1^{++}, so that it has an S-wave coupling to $D^{*0}\bar{D}^0$ and $D^0\bar{D}^{*0}$. In this case, the measured mass M_X implies unambiguously that X must be either a charm meson molecule or a virtual state of charm mesons. The remaining challenge is to discriminate between these two possibilities. The Belle Collaboration has set an upper bound on the width of the X: $\Gamma_X < 2.3$ MeV at the 90% confidence level [1]. If the width of the X is sufficiently small, there is a clear qualitative difference in the line shapes of X between these two possibilities. We first consider the $D^0\bar{D}^0\pi^0$ decay mode, which has a contribution from the decay of a constituent D^{*0}. If the X was a charm meson molecule, its line shape in $D^0\bar{D}^0\pi^0$ would consist of a Breit-Wigner resonance below the $D^{*0}\bar{D}^0$ threshold and a threshold enhancement above the $D^{*0}\bar{D}^0$ threshold. If the X was a virtual state, there would only be the threshold enhancement above the $D^{*0}\bar{D}^0$ threshold. We next consider decay modes that have no contributions from the decay of a constituent D^{*0}, such as $J/\psi\pi^+\pi^-$. If the X was a charm meson molecule, its line shape in such a decay mode would be a Breit-Wigner resonance below the $D^{*0}\bar{D}^0$ threshold. If the X was a virtual state, there would only be a cusp at the $D^{*0}\bar{D}^0$ threshold. The possibility of interpreting the $X(3872)$ as a cusp at the $D^{*0}\bar{D}^0$ threshold has been suggested by Bugg [24]. Increasing the width of the X provides additional smearing of the line shapes. This makes the qualitative difference between the line shapes of a charm meson molecule and a virtual state less dramatic. To discriminate between these two possibilities therefore requires a quantitative analysis.

The proposal that $X(3872)$ is a charm meson virtual state has received support from a recent analysis by Hanhart *et al.* [25] of data on $B^+ \to K^+ + J/\psi\pi^+\pi^-$ and $B^+ \to K^+ + D^0\bar{D}^0\pi^0$ from the Belle and *BABAR* Collaborations. They concluded that the $D^0\bar{D}^0\pi^0$ threshold enhancement is compatible with the $X(3872)$ only if it is a virtual state. One flaw in the analysis of Ref. [25] is that they did not take into account the width of the constituent D^{*0}. They identified the rate for $D^0\bar{D}^0\pi^0$ with the rate for $D^{*0}\bar{D}^0$ and $D^0\bar{D}^{*0}$ multiplied by the 62% branching fraction for $D^{*0} \to D^0\pi^0$. Thus they assumed that $D^0\bar{D}^0\pi^0$ could not be produced below the $D^{*0}\bar{D}^0$ threshold. Since a bound state has energy below the threshold, this implies that X cannot decay into $D^0\bar{D}^0\pi^0$ if it is a bound state. This contradicts one of the universal features of an S-wave threshold resonance. As the binding energy of the resonance decreases, the mean separation of the constituents grows increasingly large, suppressing all decay modes except those from the decay of a constituent.

In this paper, we develop a simple approximation to the line shapes of the $X(3872)$ that takes into account the D^{*0} width. In Sec. II, we analyze the decays of the D^* mesons and give a simple expression for the energy-dependent width of a virtual D^{*0}. In Sec. III, we give an expression for the scattering amplitude for $D^{*0}\bar{D}^0$ that takes into account the width of the D^{*0} as well as inelastic scattering channels for the charm mesons. In Sec. IV, we use that scattering amplitude together with the factorization methods of Refs. [19,21] to derive the line shapes of $X(3872)$ in the decays $B^+ \to K^+ + X$. In Sec. V, we give an order-of-magnitude estimate of the short-distance factor associated with the $B^+ \to K^+$ transition in the factorization formula. In Sec. VI, we discuss the analysis of Ref. [25] and point out the flaw from neglecting the effects of the D^{*0} width. In Sec. VII, we carry out a new analysis of the data on $B^+ \to K^+ + J/\psi\pi^+\pi^-$ and $B^+ \to K^+ + D^0\bar{D}^0\pi^0$ from the Belle Collaboration, taking into account the effects of the D^{*0} width. In Sec. VIII, we discuss ways in which our description for the line shapes could be further improved.

II. D^* WIDTHS

In this section, we present a quantitative analysis of the decay widths of the D^* mesons. There are particles with six different masses that enter into the analysis. We therefore introduce concise notation for the masses of the charm mesons and the pions. We denote the masses of the spin-0 charm mesons D^0 and D^+ by M_0 and M_1, respectively. We denote the masses of the spin-1 charm mesons D^{*0} and D^{*+} by M_{*0} and M_{*1}, respectively. We denote the masses of the pions π^0 and π^+ by m_0 and m_1, respectively. In each case, the numerical subscript is the absolute value of the electric charge of the meson. The pion mass scale corresponding to either m_0 or m_1 will be denoted by m_π. The result of a recent precision measurement of the D^0 mass by the CLEO Collaboration is $M_0 = 1864.85 \pm 0.18$ MeV,

where we have combined the errors in quadrature [10]. We use the PDG values for the differences between the charm meson masses [9]. The errors on the pion masses are negligible compared to those on the charm meson masses. It is also convenient to introduce concise notations for simple combinations of the masses. We denote the reduced mass of a spin-1 charm meson and a spin-0 charm meson by

$$M_{*ij} = \frac{M_{*i} M_j}{M_{*i} + M_j}. \tag{3}$$

We denote the reduced mass of a pion and a spin-0 charm meson by

$$m_{ij} = \frac{m_i M_j}{m_i + M_j}. \tag{4}$$

The phase space available for the decay $D^* \to D\pi$ depends sensitively on the difference between the D^* mass and the $D\pi$ thresholds:

$$\delta_{ijk} = M_{*i} - M_j - m_k. \tag{5}$$

The differences between the D^* masses and the thresholds for $D\pi$ states with the same electric charge are

$$\delta_{000} = 7.14 \pm 0.07 \text{ MeV}, \tag{6a}$$
$$\delta_{011} = -2.23 \pm 0.12 \text{ MeV}, \tag{6b}$$
$$\delta_{110} = 5.66 \pm 0.10 \text{ MeV}, \tag{6c}$$
$$\delta_{101} = 5.85 \pm 0.01 \text{ MeV}. \tag{6d}$$

The T-matrix elements for the decays $D^* \to D\pi$ are proportional to the dot product of the polarization vector of the D^* and the 3-momentum of the π. The coefficient of the dot product can be expressed as the product of a constant, which we denote by $\sqrt{3/2}g/f_\pi$, and a Clebsch-Gordan coefficient. The partial widths for the decays $D^* \to D\pi$ are

$$\Gamma[D^{*+} \to D^0\pi^+] = \frac{2\sqrt{2}g^2}{3\pi f_\pi^2} m_{10}^{5/2} \delta_{101}^{3/2}, \tag{7a}$$
$$\Gamma[D^{*+} \to D^+\pi^0] = \frac{\sqrt{2}g^2}{3\pi f_\pi^2} m_{01}^{5/2} \delta_{110}^{3/2}, \tag{7b}$$
$$\Gamma[D^{*0} \to D^0\pi^0] = \frac{\sqrt{2}g^2}{3\pi f_\pi^2} m_{00}^{5/2} \delta_{000}^{3/2}. \tag{7c}$$

Since $\delta_{011} < 0$, D^{*0} does not decay into $D^+\pi^-$.

The PDG value for the total width of the D^{*+} is $\Gamma[D^{*+}] = 96 \pm 22$ keV [9]. We can use the PDG values for the branching fractions for $D^{*+} \to D^+\pi^0$, $D^{*+} \to D^0\pi^+$, and $D^{*+} \to D^+\gamma$ to determine the partial widths for those decays:

$$\Gamma[D^{*+} \to D^0\pi^+] = 65.0 \pm 14.9 \text{ keV}, \tag{8a}$$
$$\Gamma[D^{*+} \to D^+\pi^0] = 29.5 \pm 6.8 \text{ keV}, \tag{8b}$$
$$\Gamma[D^{*+} \to D^+\gamma] = 1.5 \pm 0.5 \text{ keV}. \tag{8c}$$

By fitting the partial widths in Eqs. (8a) and (8b) to the expressions in Eqs. (7a) and (7b), we obtain consistent determinations of the constant g/f_π. The more accurate of the two determinations comes from the decay $D^{*+} \to D^0\pi^+$: $g/f_\pi = (2.82 \pm 0.32) \times 10^{-4}$ MeV$^{-3/2}$. Inserting this value into Eq. (7b), we can predict the partial width for $D^{*0} \to D^0\pi^0$:

$$\Gamma[D^{*0} \to D^0\pi^0] = 40.5 \pm 9.3 \text{ keV}. \tag{9}$$

By combining this prediction with the PDG value for the branching fraction for $D^{*0} \to D^0\pi^0$, we obtain a prediction for the total width of the D^{*0}: $\Gamma[D^{*0}] = 65.5 \pm 15.4$ keV. We can then predict the partial width for the decay $D^{*0} \to D^0\gamma$ using the PDG value for its branching fraction:

$$\Gamma[D^{*0} \to D^0\gamma] = 25.0 \pm 6.2 \text{ keV}. \tag{10}$$

Since the decay rates for $D^* \to D\pi$ in Eqs. (7) scale like the 3/2 power of the energy difference between the D^* mass and the $D\pi$ threshold, they are fairly sensitive to the mass of the D^*. A virtual D^{*0} with energy $M_{*0} + E$ can be considered as a D^{*0} whose rest energy differs from its physical mass by the energy E. The width of the virtual particle varies with E. We denote the energy-dependent width of the D^{*0} by $\Gamma_{*0}(E)$. If $|E|$ is small compared to the pion mass, the energy-dependent width can be obtained simply by scaling the physical partial width for the decay $D^{*0} \to D^0\pi^0$:

$$\begin{aligned}\Gamma_{*0}(E) = \Gamma[D^{*0} \to D^0\gamma] + \Gamma[D^{*0} \to D^0\pi^0][\\ \times [(\delta_{000} + E)/\delta_{000}]^{3/2} \theta(\delta_{000} + E) \\ + 2(m_{11}/m_{00})^{5/2} [(\delta_{011} + E)/\delta_{000}]^{3/2} \theta(\delta_{011} + E)].\end{aligned} \tag{11}$$

We ignore any energy dependence of the decay widths into

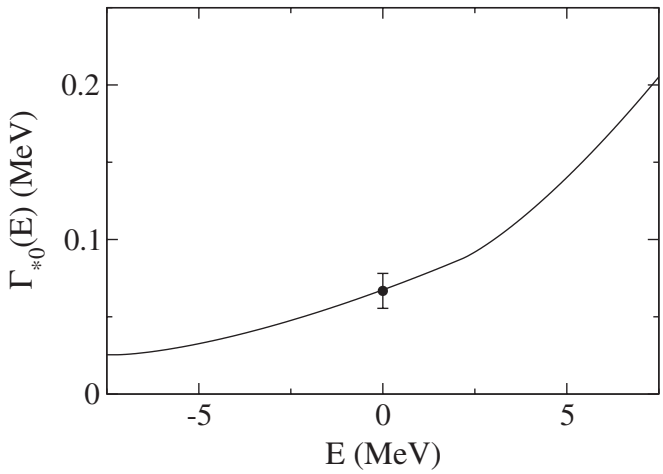

FIG. 1. The energy-dependent width $\Gamma_{*0}(E)$ of a virtual D^{*0} as a function of the energy E relative to the D^{*0} mass. The point with error bars at $E = 0$ indicates the value and uncertainty of the predicted width of D^{*0}.

$D^0\gamma$, because the photon energy and the phase space for the decays $D^{*0} \to D^0\gamma$ do not vary dramatically in the $D^{*0}\bar{D}^0$ threshold region. In Fig. 1, we plot the energy-dependent width of the D^{*0} as a function of the energy E relative to the D^{*0} mass. The three terms in Eq. (11) have obvious interpretations as energy-dependent partial widths for decays of D^{*0} into $D^0\gamma$, $D^0\pi^0$, and $D^+\pi^-$. We define energy-dependent branching fractions $\mathrm{Br}_{00\gamma}(E)$, $\mathrm{Br}_{000}(E)$, and $\mathrm{Br}_{011}(E)$ by dividing these terms by $\Gamma_{*0}(E)$. For example, the energy-dependent branching fraction for $D^{*0} \to D^0\pi^0$ is

$$\mathrm{Br}_{000}(E) = \frac{\Gamma[D^{*0} \to D^0\pi^0]}{\Gamma_{*0}(E)}[(\delta_{000} + E)/\delta_{000}]^{3/2} \times \theta(\delta_{000} + E). \tag{12}$$

III. LOW-ENERGY $D^{*0}\bar{D}^0$ SCATTERING

In this section, we discuss the low-energy scattering of the charm mesons D^{*0} and $\bar{D}^0$. The existence of the $X(3872)$ with quantum numbers 1^{++} implies that there is an S-wave resonance near threshold in the channel with even charge conjugation:

$$(D^*\bar{D})^0_+ \equiv \tfrac{1}{\sqrt{2}}(D^{*0}\bar{D}^0 + D^0\bar{D}^{*0}). \tag{13}$$

The isospin splittings between the charm meson masses are approximately 4.8 MeV for $D^+ - D^0$ and 3.3 MeV for $D^{*+} - D^{*0}$. The energy splitting between the $D^{*+}D^-$ and $D^{*0}\bar{D}^0$ thresholds is the sum of these isospin splittings:

$$\nu = 8.08 \pm 0.12 \text{ MeV}. \tag{14}$$

We will use approximations that are valid when the energy E relative to the $D^{*0}\bar{D}^0$ threshold is small compared to ν. Thus the relative momenta of the charm mesons is required to be small compared to $(2M_{*00}\nu)^{1/2} \approx 125$ MeV. This is numerically comparable to the pion mass scale: $m_\pi \approx 135$ MeV.

The presence of the $X(3872)$ resonance so close to the $D^{*0}\bar{D}^0$ threshold with quantum numbers that allow S-wave couplings to $D^{*0}\bar{D}^0$ and $D^0\bar{D}^{*0}$ indicates that it is necessary to treat the interaction that produces the resonance nonperturbatively in order to take into account the constraints of unitarity. The resonance is in the channel $(D^*\bar{D})^0_+$. There may also be scattering in the channel that is odd under charge conjugation, but we will assume that it can be neglected compared to scattering in the resonant channel. Since the kinetic energy is so low, the scattering will be predominantly S-wave.

We express the transition amplitude $\mathcal{A}(E)$ for the scattering of nonrelativistically normalized charm mesons in the channel $(D^*\bar{D})^0_+$ in the form

$$\mathcal{A}(E) = \frac{2\pi}{M_{*00}} f(E), \tag{15}$$

where $f(E)$ is the conventional nonrelativistic scattering amplitude. An expression for the low-energy scattering amplitude with an S-wave threshold resonance that is compatible with unitarity is

$$f(E) = \frac{1}{-\gamma + \kappa(E)}, \tag{16}$$

where $\kappa(E) = (-2M_{*00}E - i\varepsilon)^{1/2}$ and E is the total energy of the charm mesons relative to the $D^{*0}\bar{D}^0$ threshold. If E is real, the variable $\kappa(E)$ is real and positive for $E < 0$ and it is pure imaginary with a negative imaginary part for $E > 0$. The parameter γ in Eq. (16) can be identified as the inverse scattering length. If γ is complex, the imaginary part of the scattering amplitude in Eq. (16) satisfies

$$\mathrm{Im}\, f(E) = |f(E)|^2 \mathrm{Im}[\gamma - \kappa(E)]. \tag{17}$$

The scattering amplitude $f(E)$ in Eq. (16) satisfies the constraints of unitarity for a single-channel system exactly provided γ is a real analytic function of E. For positive real values of the energy E, Eq. (17) is simply the optical theorem for this single-channel system:

$$\mathrm{Im}\, f(E) = |f(E)|^2\sqrt{2M_{*00}E} \qquad (E > 0). \tag{18}$$

The left side is the imaginary part of the T-matrix element for elastic scattering in the $(D^*\bar{D})^0_+$ channel. The right side is the cross section for elastic scattering multiplied by $[E/(2M_{*00})]^{1/2}$. If $\gamma > 0$, the amplitude $f(E)$ has a pole at a negative value of the energy E, indicating the existence of a stable bound state. If γ varies sufficiently slowly with E, we can approximate it by a constant. The pole is then at $E_{\mathrm{pole}} \approx -\gamma^2/(2M_{*00})$ and the binding energy is $\gamma^2/(2M_{*00})$. In addition to the contribution to the imaginary part of $f(E)$ in Eq. (18), there is a delta-function contribution at $E = E_{\mathrm{pole}}$:

$$\mathrm{Im}\, f(E) \approx \frac{\pi\gamma}{M_{*00}}\delta(E + \gamma^2/(2M_{*00})) \qquad (E < 0,\ \gamma > 0). \tag{19}$$

If $\gamma < 0$, the pole in the amplitude $f(E)$ is not on the real E axis, but on the second sheet of the complex variable E. The standard terminology for such a pole is a *virtual state*. The imaginary part of the amplitude is nonzero only in the positive E region and is given by Eq. (18).

We would like to identify the bound state in the case $\gamma > 0$ with the $X(3872)$. However, since the X decays, it must have a nonzero width. Its decay modes include $D^0\bar{D}^0\pi^0$ and $D^0\bar{D}^0\gamma$, which receive contributions from decays of the constituent D^{*0} or $\bar{D}^{*0}$. There are also other decay modes, including $J/\psi\pi^+\pi^-$, $J/\psi\pi^+\pi^-\pi^0$, and $J/\psi\gamma$. All the decay modes of X are inelastic scattering channels for the charm mesons. The dominant effects of these inelastic scattering channels on scattering in the $(D^*\bar{D})^0_+$ channel can be taken into account through simple modifications of the variables γ and $\kappa(E)$ in the resonant amplitude $f(E)$ in Eq. (16). The effects of the decays of the

constituent D^{*0} or $\bar{D}^{*0}$ can be taken into account simply by replacing the mass M_{*0} that is implicit in the energy E measured from the $D^{*0}\bar{D}^0$ threshold by $M_{*0} - i\Gamma_{*0}(E)/2$, where $\Gamma_{*0}(E)$ is the energy-dependent width of the D^{*0} given in Eq. (11). This changes the energy variable $\kappa(E)$ defined after Eq. (16) to

$$\kappa(E) = \sqrt{-2M_{*00}[E + i\Gamma_{*0}(E)/2]}. \tag{20}$$

At the threshold $E = 0$, the energy-dependent width $\Gamma_{*0}(E)$ reduces to the physical width $\Gamma[D^{*0}]$. The expression for $\kappa(E)$ in Eq. (20) requires a choice of branch cut for the square root. If E is real, an explicit expression for $\kappa(E)$ that corresponds to the appropriate choice of branch cut can be obtained by using the identity

$$\sqrt{-2M[E + i\Gamma/2]} = \sqrt{M}[(\sqrt{E^2 + \Gamma^2/4} - E)^{1/2} - i(\sqrt{E^2 + \Gamma^2/4} + E)^{1/2}]. \tag{21}$$

The effects of inelastic channels other than $D^0\bar{D}^0\pi^0$ and $D^0\bar{D}^0\gamma$ on scattering in the $(D^*\bar{D})^0_+$ channel can be taken into account by replacing the real parameter γ in Eq. (16) by a complex parameter with a positive imaginary part. With these modifications of the variables γ and $\kappa(E)$, the expression for the imaginary part of the amplitude $f(E)$ in Eq. (17) can now be interpreted as the optical theorem for this multichannel system. The right side can be interpreted as the total cross section for scattering in the $(D^*\bar{D})^0_+$ channel multiplied by $[E/(2M_{*00})]^{1/2}$. The term proportional to $\mathrm{Im}\,\gamma$ can be interpreted as the contribution from the inelastic scattering channels. This interpretation requires $\mathrm{Im}\,\gamma > 0$. The term proportional to $-\mathrm{Im}\,\kappa(E)$ includes a contribution that reduces to the right side of Eq. (18) in the limits $\mathrm{Im}\,\gamma \to 0$ and $\Gamma_{*0} \to 0$. It can be interpreted as due to elastic scattering into $D^{*0}\bar{D}^0$ or $D^0\bar{D}^{*0}$. If $\mathrm{Re}\gamma > 0$, the term proportional to $-\mathrm{Im}\,\kappa(E)$ also includes a contribution that reduces to the right side of Eq. (18) in the limits $\mathrm{Im}\,\gamma \to 0$ and $\Gamma_{*0} \to 0$. It can interpreted as due to scattering into the X resonance. The D^{*0} or $\bar{D}^{*0}$ produced by the elastic scattering process will eventually decay. Similarly, the constituent D^{*0} or $\bar{D}^{*0}$ in the X resonance will eventually decay. Thus the ultimate final states corresponding to the term proportional to $-\mathrm{Im}\,\kappa(E)$ in Eq. (17) can be identified as $D^0\bar{D}^0\pi^0$ and $D^0\bar{D}^0\gamma$, and also $D^+\bar{D}^0\pi^-$ and $D^0D^-\pi^+$ if the energy E exceeds the threshold $|\delta_{011}| = 2.2$ MeV.

The scattering amplitude $f(E)$ given by Eqs. (16) and (20) is a double-valued function of the complex energy E with a square-root branch point and a pole. If we neglect the energy dependence of the width $\Gamma_{*0}(E)$, the branch point is near $E = -i\Gamma[D^{*0}]/2$ and the position of the pole is

$$E_{\mathrm{pole}} \approx -\frac{\gamma^2}{2M_{*00}} - \frac{i}{2}\Gamma[D^{*0}]. \tag{22}$$

If $\mathrm{Re}\gamma > 0$, the pole is on the physical sheet of the energy E. It can be expressed in the form

$$E_{\mathrm{pole}} = -E_X - i\Gamma_X/2, \tag{23}$$

where E_X and Γ_X are given by

$$E_X \approx [(\mathrm{Re}\gamma)^2 - (\mathrm{Im}\,\gamma)^2]/(2M_{*00}), \tag{24a}$$

$$\Gamma_X \approx \Gamma[D^{*0}] + 2(\mathrm{Re}\gamma)(\mathrm{Im}\,\gamma)/M_{*00}. \tag{24b}$$

If $E_X > 0$ and $\Gamma_X \ll E_X$, the state X is a resonance whose line shape in the region $|E - E_X| \ll E_X$ is a Breit-Wigner resonance centered at energy $-E_X$ with full width at half maximum Γ_X. If Γ_X is not small compared to E_X, one can choose to define the binding energy and the width of X to be given by the expressions for E_X and Γ_X in Eqs. (24), but they should not be interpreted literally. If $\mathrm{Re}\gamma < 0$, the pole at the energy E_{pole} in Eq. (22) is on the second sheet of the energy E and it corresponds to a virtual state. In this case, the expressions for E_X and Γ_X in Eqs. (24) have no simple physical interpretations.

IV. LINE SHAPES OF $X(3872)$ IN B^+ DECAY

If a set of particles C has total quantum numbers that are compatible with those of the $X(3872)$ resonance and if the total energy E of these particles is near the $D^{*0}\bar{D}^0$ threshold, then there will be a resonance in the channel C. The line shape of $X(3872)$ in the channel C is the differential rate as a function of the total energy E of the particles in C. In this section, we discuss the line shapes of the $X(3872)$ for energy E close enough to the $D^{*0}\bar{D}^0$ threshold that we need only consider the resonant channel $(D^*\bar{D})^0_+$ defined in Eq. (13). This requires $|E|$ to be small compared to the energy $\nu \approx 8.1$ MeV of the $D^{*+}D^-$ threshold.

In Ref. [19], it was pointed out that the line shape for decay modes of X that do not involve decays of a constituent can be factored into short-distance factors that are insensitive to E and to the inverse scattering length γ and a resonance factor that depends dramatically on E and γ. In Ref. [21], it was shown that the factorization formulas could be derived using the operator product expansion for an effective field theory that describes the $c\bar{c}$ sector of QCD near the $D^{*0}\bar{D}^0$ threshold. The factorization formulas hold for any *short-distance* process, which we define to be one in which all the particles in the initial state and all the particles in the final state beside the resonating particles have momenta in the resonance rest frame that are of order m_π or larger. An example of a short-distance process is the discovery mode $B^+ \to K^+ + J/\psi\pi^+\pi^-$. In the $J/\psi\pi^+\pi^-$ rest frame, the momenta of the B^+ and K^+ are 1555 MeV, which is much larger than m_π. The root-mean-square momentum of the J/ψ in the $J/\psi\pi^+\pi^-$ rest frame is 319 MeV, which is significantly larger than m_π.

We consider the short-distance process $B^+ \to K^+ + C$ in which the collection of particles denoted by C have a resonant enhancement associated with the $X(3872)$. If the

total energy E of the particles in C is near the $D^{*0}\bar{D}^0$ threshold, the amplitude for the process $B^+ \to K^+ + C$ factors into a short-distance factor associated with the process $B^+ \to K^+ + (D^*\bar{D})^0_+$, a resonance factor $f(E)$ given by Eq. (16), and a short-distance factor associated with the process $(D^*\bar{D})^0_+ \to C$. Since the short-distance factors are insensitive to E, the only dramatic dependence on E comes from the factor $f(E)$. Thus the line shape $d\Gamma/dE$ is proportional to $|f(E)|^2$.

For an alternative derivation of this line shape that also gives the line shapes for $D^0\bar{D}^0\pi^0$ and $D^0\bar{D}^0\gamma$, we consider the inclusive differential decay rate into all channels that are enhanced by the $(D^*\bar{D})^0_+$ resonance. Using cutting rules, the inclusive decay rate in the region near the $D^{*0}\bar{D}^0$ threshold summed over all resonant channels can be expressed in the form

$$\frac{d\Gamma}{dE}[B^+ \to K^+ + \text{resonant}] = 2\Gamma^{K^+}_{B^+} \,\text{Im}\, f(E), \tag{25}$$

where $\Gamma^{K^+}_{B^+}$ is a short-distance factor defined in Ref. [21]. The optical theorem in Eq. (17) can be used to resolve this inclusive resonant rate into two terms. We interpret the term proportional to $\text{Im}\,\gamma$ as the sum of all contributions from short-distance channels. Thus the line shape of $X(3872)$ in a specific short-distance channel C can be expressed as

$$\frac{d\Gamma}{dE}[B^+ \to K^+ + C] = 2\Gamma^{K^+}_{B^+}|f(E)|^2\Gamma^C(E), \tag{26}$$

where $\Gamma^{K^+}_{B^+}$ is the same short-distance factor as in Eq. (25) and $\Gamma^C(E)$ is a short-distance factor associated with the transition of the charm mesons to the particles in C. The factor $\Gamma^C(E)$ in Eq. (26) differs by a factor of π from the factor Γ^C defined in Ref. [21]. With this convention, $\Gamma^C(E)$ is the contribution of the state C to the term $\text{Im}\gamma$ in Eq. (17). As indicated by the argument E, we have allowed for the possibility that the dependence of this term on E is not negligible in the $D^{*0}\bar{D}^0$ threshold region. The justification for Eq. (26) relies on first order perturbation theory in the coupling to the channel C. If that coupling is too large, the channels $(D^*\bar{D})^0_+$ and C would have to be treated as a two-channel resonating system. In the case of the channel $J/\psi\pi^+\pi^-$, first order perturbation theory can be justified by the small branching ratio of the decay of X into $J/\psi\pi^+\pi^-$ relative to $D^0\bar{D}^0\pi^0$ measured by the Belle Collaboration [8].

We interpret the term proportional to $-\text{Im}\,\kappa(E)$ in Eq. (17) as the sum of all contributions from channels that correspond to $D^{*0}\bar{D}^0$ or $D^0\bar{D}^{*0}$ followed by the decay of the D^{*0} or $\bar{D}^{*0}$. We can further resolve this term into the contributions from the channels $D^0\bar{D}^0\pi^0$, $D^0\bar{D}^0\gamma$, $D^+\bar{D}^0\pi^-$, and $D^0D^-\pi^+$ by multiplying it by the energy-dependent branching fractions $\text{Br}_{000}(E)$, $\text{Br}_{00\gamma}(E)$, $\frac{1}{2}\text{Br}_{011}(E)$, and $\frac{1}{2}\text{Br}_{011}(E)$, which add up to 1. A simple expression for $-\text{Im}\,\kappa(E)$ can be obtained by using the identity in Eq. (21). The resulting expression for the line shape of X in the $D^0\bar{D}^0\pi^0$ channel is

$$\frac{d\Gamma}{dE}[B^+ \to K^+ + D^0\bar{D}^0\pi^0] = 2\Gamma^{K^+}_{B^+}|f(E)|^2 \times [M_{*00}(\sqrt{E^2 + \Gamma_{*0}(E)^2/4} + E)]^{1/2}\text{Br}_{000}(E), \tag{27}$$

where $\Gamma^{K^+}_{B^+}$ is the same short-distance factor as in Eq. (25) and $\text{Br}_{000}(E)$ is given in Eq. (12).

In Ref. [20], the decay rates of X into J/ψ plus pions and photons were calculated under the assumption that these decays proceed through couplings of the X to J/ψ and the vector mesons ρ^0 and ω. The results of Ref. [20] can be used to calculate the dependence of the factor $\Gamma^C(E)$ in Eq. (26) on the energy E for $C = J/\psi\pi^+\pi^-$, $J/\psi\pi^+\pi^-\pi^0$, $J/\psi\pi^0\gamma$, and $J/\psi\gamma$. The normalization of this factor, which we can take to be $\Gamma^C(0)$, can only be determined by measurements of the branching fraction of $X(3872)$ into the final state C. In Fig. 2, we plot the energy dependence of the factors $\Gamma^C(E)$ for $C = J/\psi\pi^+\pi^-$ and $J/\psi\pi^+\pi^-\pi^0$. The larger variations for $J/\psi\pi^+\pi^-\pi^0$ are due to the width of ω being much smaller than that of ρ^0. Very close to the threshold, the final-state factors can be approximated by the expressions

$$\Gamma^{J/\psi\pi^+\pi^-}(E) \approx (1 + a_2 E)\Gamma^{\psi 2\pi}_0, \tag{28a}$$

$$\Gamma^{J/\psi\pi^+\pi^-\pi^0}(E) \approx (1 + a_3 E)\Gamma^{\psi 3\pi}_0, \tag{28b}$$

where the coefficients are $a_2 = 0.0175\ \text{MeV}^{-1}$ and $a_3 = 0.0809\ \text{MeV}^{-1}$. The approximations in Eqs. (28a) and (28b) are accurate to within 1% for $-8.5\ \text{MeV} < E < 10.1\ \text{MeV}$ and $-4.3\ \text{MeV} < E < 1.0\ \text{MeV}$, respectively.

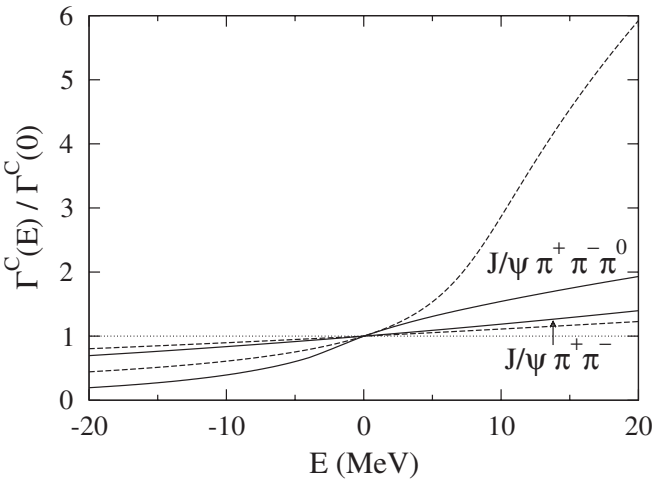

FIG. 2. Energy dependence of the final-state factors $\Gamma^C(E)$ for the channels $C = J/\psi\pi^+\pi^-$ and $J/\psi\pi^+\pi^-\pi^0$. The factors $\Gamma^C(E)/\Gamma^C(0)$ as functions of the energy E relative to the $D^{*0}\bar{D}^0$ threshold are shown as solid curves. The dashed curves are the corresponding factors used in Ref. [25].

In Fig. 2, we also show the energy dependence of the factors analogous to $\Gamma^C(E)$ that were used in Ref. [25]. Those factors were denoted by $\Gamma_{\pi^+\pi^- J/\psi}(E)/g$ and $\Gamma_{\pi^+\pi^-\pi^0 J/\psi}(E)/g$. In Ref. [25], the $\pi^+\pi^-$ and $\pi^+\pi^-\pi^0$ systems were treated simply as Breit-Wigner resonances with the masses and widths of the ρ^0 and ω. The additional dependence on E from the coupling of the resonances to pions and from the integration over the phase space of the pions was not taken into account. In the region $|E| < 1$ MeV, the factors in Ref. [25] analogous to $\Gamma^C(E)/\Gamma^C(0)$ differ from ours by less than 1.4% for $C = J/\psi\pi^+\pi^-$ and by less than 2.4% for $C = J/\psi\pi^+\pi^-\pi^0$. As illustrated in Fig. 2, the differences are more substantial when $|E|$ is 10 MeV or larger and they are particularly large for $J/\psi\pi^+\pi^-\pi^0$.

In Fig. 3, we illustrate the line shapes of $X(3872)$ in the $D^0\bar{D}^0\pi^0$ channel and in a short-distance channel, such as $J/\psi\pi^+\pi^-$. We take the parameter γ to be real, which corresponds to the assumption that decay modes other than $D^0\bar{D}^0\pi^0$ and $D^0\bar{D}^0\gamma$ give a small contribution to the total width of $X(3872)$. In Fig. 3, the solid lines are the line shapes for a short-distance decay mode, which is given by Eq. (26). We neglect the energy dependence from the factor $\Gamma^C(E)$, which is very small for $J/\psi\pi^+\pi^-$. The dashed lines are the line shapes for $D^0\bar{D}^0\pi^0$, which is given by Eq. (27). We show the line shapes for five values of γ: 48, 34, 0, -34, and -48 MeV. For $\gamma = 34$, 0, and 48 MeV, the peaks of the resonance are at $E = -0.6$, 0, and -1.2 MeV, respectively. They correspond to the central value of the measurement in Eq. (1) and deviations by $\pm 1\sigma$ from the central value. In Fig. 3, the line shapes for the short-distance channel and for the $D^0\bar{D}^0\pi^0$ channel are separately normalized so that the maximum value is 1 for $\gamma = 0$. This figure illustrates that as γ decreases toward 0 from above, the area under the short-distance line shape decreases and it becomes very small for negative values of γ. As γ decreases toward 0 from above, the area under the $D^0\bar{D}^0\pi^0$ line shape decreases less rapidly, but it is also small for negative values of γ. At the values $\gamma = 48$, 34, 0, -34, and -48 MeV, the differences between the positions of the peaks in the $D^0\bar{D}^0\pi^0$ channel and the short-distance channel are 0.000 24, 0.000 52, 0.019, 0.75, and 1.75 MeV, respectively. Thus the $4.7^{+1.0}_{-1.8}$ MeV difference between the masses in Eqs. (1) and (2) appears to be only compatible with negative values of γ.

In an actual measurement, the line shapes shown in Fig. 3 would be smeared by the effects of experimental resolution. In the Belle discovery paper, the $X(3872)$ signal in $J/\psi\pi^+\pi^-$ was fit by a Gaussian with width 2.5 MeV, which is compatible with the experimental resolution [1]. For the $D^0\bar{D}^0\pi^0$ enhancement near threshold, the signal was fit by a Gaussian with width 2.24 MeV, which is again compatible with the experimental resolution [5]. In Fig. 4, we illustrate the effects of experimental resolution by smearing the line shapes in Fig. 3 by a Gaussian with width 2.5 MeV. At the values $\gamma = 48$, 34, 0, -34, and -48 MeV, the differences between the positions of the peaks in the $D^0\bar{D}^0\pi^0$ channel and the short-distance channel are 0.45, 0.82, 2.0, 2.4, and 3.2 MeV, respectively. Thus, after taking into account the effects of experimental resolution, the $4.7^{+1.0}_{-1.8}$ MeV difference between the masses in Eqs. (1) and (2) is not incompatible with a positive value of γ.

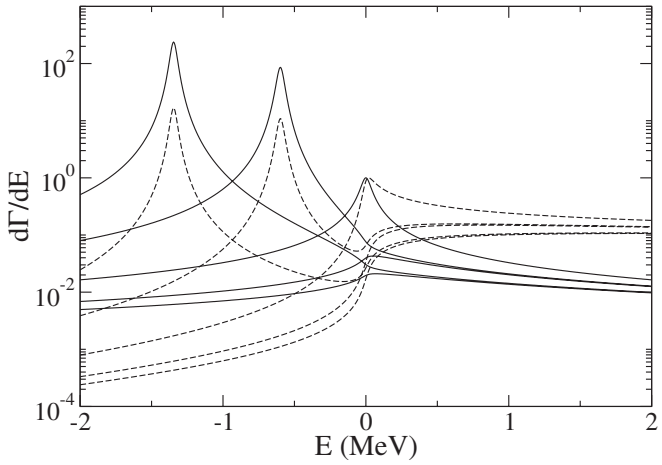

FIG. 3. The line shapes in a short-distance channel (solid lines) and in the $D^0\bar{D}^0\pi^0$ channel (dashed lines). The line shapes are shown for five values of γ: -48, -34, 0, 34, and 48 MeV. The line shapes in the short-distance channel and in the $D^0\bar{D}^0\pi^0$ channel are separately normalized so that the curve for $\gamma = 0$ has a maximum value of 1. At $E = 0.2$ MeV, the order of both the solid curves and the dashed curves from top to bottom is $\gamma =$ 0, 34, -34, 48, and -48 MeV.

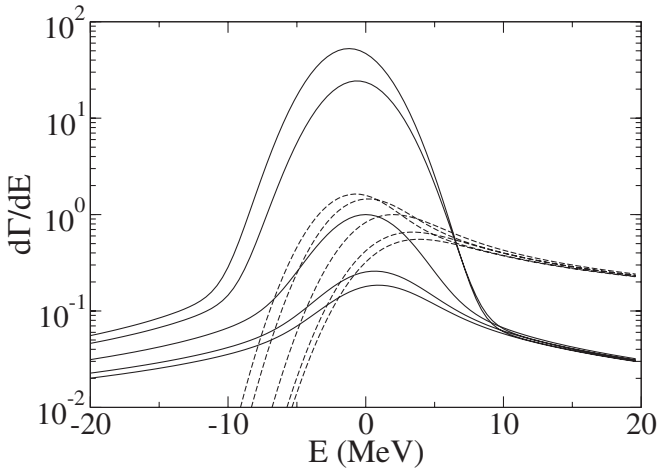

FIG. 4. Same as in Fig. 3, except that the line shapes have been smeared by a Gaussian function with width 2.5 MeV to mimic the effects of experimental resolution. The smeared line shapes in the short-distance channel and in the $D^0\bar{D}^0\pi^0$ channel are separately normalized so that the curve for $\gamma = 0$ has a maximum value of 1. At $E = 0$ MeV, the order of both the solid curves and the dashed curves from top to bottom is $\gamma = 48$, 34, 0, -34, and -48 MeV.

V. ESTIMATE OF THE SHORT-DISTANCE FACTOR

In this section, we give an order-of-magnitude estimate of the short-distance factor $\Gamma_{B^+}^{K^+}$ that appears in Eqs. (25)–(27). We use the measurement by the *BABAR* Collaboration of the branching fraction for the decay of B^+ into $K^+D^{*0}\bar{D}^0$ [26]:

$$\mathrm{Br}[B^+ \to K^+ D^{*0}\bar{D}^0] = (4.7 \pm 1.0) \times 10^{-3}. \tag{29}$$

The upper bound on the branching fraction for $K^+D^0\bar{D}^{*0}$ is 3.7×10^{-3} at the 90% confidence level. The partial width for the decay in Eq. (29) can be written

$$\Gamma[B^+ \to K^+ D^{*0}\bar{D}^0] = \frac{3}{2M_B}\langle|\mathcal{M}|^2\rangle \Phi_{B^+}^{K^+D^{*0}\bar{D}^0}, \tag{30}$$

where $\Phi_{B^+}^{K^+D^{*0}\bar{D}^0} = 194.5\ \mathrm{MeV}^2$ is the integral of the three-body phase space and $3\langle|\mathcal{M}|^2\rangle$ is the square of the matrix element averaged over the relativistic three-body phase space and summed over the D^{*0} spins. Using the measured lifetime, $\tau[B^+] = 1.64 \times 10^{-12}$ s, and the central value of the branching fraction in Eq. (29), we find that the average value of the square of the matrix element in Eq. (30) is $\langle|\mathcal{M}|^2\rangle = 3.4 \times 10^{-11}$.

The differential rate for B^+ to decay into $K^+ + D^{*0}\bar{D}^0$ with $D^{*0}\bar{D}^0$ near its threshold can be written

$$\frac{d\Gamma}{dE}[B^+ \to K^+ + D^{*0}\bar{D}^0] = \frac{3\lambda^{1/2}(M_B, M_{*0} + M_0, m_K)}{64\pi^3 M_B^3} \times |\mathcal{M}|^2\sqrt{2M_{*00}E}, \tag{31}$$

where E is the rest energy of the $D^{*0}\bar{D}^0$ relative to its threshold and $|\mathcal{M}|^2$ is the square of the matrix element averaged over angles in the $D^{*0}\bar{D}^0$ rest frame and averaged over the D^{*0} spins. The dramatic dependence of $|\mathcal{M}|^2$ on E comes from the resonance factor $|f(E)|^2$ in Eq. (27). By comparing Eq. (31) with Eq. (27), we can obtain an expression for the short-distance factor $\Gamma_{B^+}^{K^+}$:

$$\Gamma_{B^+}^{K^+} = \frac{3\lambda^{1/2}(M_B, M_{*0} + M_0, m_K)}{128\pi^3 M_B^3} \lim_{E\to 0}|\mathcal{M}|^2/|f(E)|^2. \tag{32}$$

Because of the threshold resonance, the square of the matrix element $|\mathcal{M}|^2$ for $B^+ \to K^+ + D^{*0}\bar{D}^0$ should be significantly larger near the $D^{*0}\bar{D}^0$ threshold than its average $\langle|\mathcal{M}|^2\rangle$ over the entire three-body phase. We will assume that this threshold resonance is the only effect that gives a significant enhancement of $|\mathcal{M}|^2$ in this corner of the phase space. Thus as an order-of-magnitude estimate of $|\mathcal{M}|^2$, we will take

$$|\mathcal{M}|^2 \approx \langle|\mathcal{M}|^2\rangle \frac{\Lambda^2}{|-\gamma + \kappa(E)|^2}, \tag{33}$$

where $\langle|\mathcal{M}|^2\rangle$ is the average value of the square of the matrix element defined by Eq. (30) and Λ is the momentum scale below which the resonant behavior sets in. The natural scale for Λ is $(2M_{*11}\nu)^{1/2} = 125$ MeV or $m_\pi = 135$ MeV. The estimate in Eq. (33) is likely to be an underestimate because $\langle|\mathcal{M}|^2\rangle$ is enhanced by various resonant contributions, including $D_{s1}(2536) + \bar{D}^0$. Using the value of $\langle|\mathcal{M}|^2\rangle$ that corresponds to the central value of the branching fraction in Eq. (29), our estimate of the short-distance factor is

$$\Gamma_{B^+}^{K^+} \approx (3.8 \times 10^{-14}\ \mathrm{MeV})\frac{\Lambda^2}{m_\pi^2}. \tag{34}$$

VI. ANALYSIS OF REF. [25]

In Ref. [25], the authors analyzed the data from the Belle and *BABAR* collaborations on $B \to K + X(3872)$ using a generalized Flatté parametrization for the $(D^*\bar{D})_+^0$ scattering amplitude:

$$f_{\mathrm{HKKN}}(E) = \Big(-\frac{2}{g}[E - E_f + i\Gamma_{\pi^+\pi^- J/\psi}(E)/2 + i\Gamma_{\pi^+\pi^-\pi^0 J/\psi}(E)/2] + \kappa(E) + \kappa_1(E)\Big)^{-1}, \tag{35}$$

where $\kappa(E) = (-2M_{*00}E + i\epsilon)^{1/2}$ and $\kappa_1(E) = (-2M_{*11}(E-\nu) + i\epsilon)^{1/2}$. The functions $\Gamma_{\pi^+\pi^- J/\psi}(E)$ and $\Gamma_{\pi^+\pi^-\pi^0 J/\psi}(E)$ are determined by the ρ and ω resonance parameters up to normalization factors f_ρ and f_ω. The resonant term in the differential branching fraction for the inclusive decay of B^+ into K^+ was expressed in the form

$$\frac{d\mathrm{Br}}{dE}[B^+ \to K^+ + \mathrm{resonant}] = \frac{2}{\pi}(\mathcal{B}/g)\mathrm{Im}\, f(E). \tag{36}$$

The adjustable parameters in the model of Ref. [25] are g, E_f, f_ρ, f_ω, and $\mathcal{B}$. The imaginary part of the scattering amplitude in Eq. (35) is

$$\mathrm{Im}\, f_{\mathrm{HKKN}}(E) = |f(E)|^2[\Gamma_{\pi^+\pi^- J/\psi}(E)/g + \Gamma_{\pi^+\pi^-\pi^0 J/\psi}(E)/g - \mathrm{Im}\,\kappa(E) - \mathrm{Im}\,\kappa_1(E)]. \tag{37}$$

The first two terms in the square brackets are identified with the contributions from $J/\psi\pi^+\pi^-$ and $J/\psi\pi^+\pi^-\pi^0$, respectively. The third term $-\mathrm{Im}\,\kappa(E)$ is nonzero only for $E > 0$ and was identified with the contribution from $D^0\bar{D}^0\pi^0$. The last term $-\mathrm{Im}\,\kappa_1(E)$ is nonzero only for $E > \nu$ and could be identified with the contributions from $D^{*+}D^-$ and D^+D^{*-}.

In the analysis of Ref. [25], the ratio f_ω/f_ρ was determined from the branching ratio of $X(3872)$ into $J/\psi\pi^+\pi^-\pi^0$ and $J/\psi\pi^+\pi^-$ measured by the Belle Collaboration [5]. The parameters g, E_f, f_ρ, and $\mathcal{B}$ were then used to fit the $J/\psi\pi^+\pi^-$ energy distributions in the decay $B^+ \to K^+ + J/\psi\pi^+\pi^-$ measured by the Belle and

BABAR Collaborations [1,27] and the $D^0\bar{D}^0\pi^0$ energy distribution in the decay $B^+ \to K^+ + D^0\bar{D}^0\pi^0$ measured by the Belle Collaboration [8]. The authors of Ref. [25] found that their fits exhibited scaling behavior. The fits were insensitive to rescaling all the parameters g, E_f, f_ρ, f_ω, and $\mathcal{B}$ by a common factor. From the expressions in Eqs. (35)–(37), one can see that the scaling behavior simply implies that the term $-(2/g)E$ in the denominator of Eq. (35) can be neglected. The authors interpreted the parameter g as a $D\bar{D}^*$ coupling constant. However a more appropriate interpretation of g is that it determines the effective range r_s for S-wave scattering in the $(D^*\bar{D})^0_+$ channel. If we neglect the small imaginary terms proportional to $\Gamma_{\pi^+\pi^- J/\psi}(E)$ and $\Gamma_{\pi^+\pi^-\pi^0 J/\psi}(E)$ in the denominator in Eq. (35), the inverse scattering length and the effective range are

$$\gamma \approx -2(E_f/g) - \sqrt{2M_{*11}\nu}, \tag{38a}$$

$$r_s \approx -2/(M_{*00}g) - 1/\sqrt{2M_{*11}\nu}. \tag{38b}$$

We have simplified the expression for r_s in Eq. (38b) by setting $M_{*11}/M_{*00} = 1$. The inverse scattering lengths γ calculated from Eq. (38a) using the parameters of the fits in Ref. [25] range from -51.7 MeV to -66.3 MeV. These values are close to the exact results for the complex inverse scattering length γ for the fits in Ref. [25]. Their real parts ranged from -48.9 MeV to -63.5 MeV and their imaginary parts ranged from 3.3 MeV to 6.8 MeV. Because of the scaling behavior, the scattering amplitude near the $D^{*0}\bar{D}^0$ threshold is insensitive to the effective range r_s, so its numerical value cannot be determined from the fits of Ref. [25]. The authors could have obtained essentially the same fits by taking the range r_s to be 0. They could have replaced the scattering amplitude in Eq. (35) by

$$f_{\mathrm{HKKN}}(E) \approx [-\mathrm{Re}\gamma - i\Gamma_{\pi^+\pi^- J/\psi}(E)/g - i\Gamma_{\pi^+\pi^-\pi^0 J/\psi}(E)/g + \kappa(E)]^{-1}, \tag{39}$$

with $\mathrm{Re}\gamma$, f_ρ/g, f_ω/g, and $\mathcal{B}/g$ as the adjustable parameters.

The authors of Ref. [25] found that they could obtain acceptable fits to the Belle and *BABAR* data only if the $J/\psi\pi^+\pi^-$ energy distribution was peaked almost exactly at the $D^{*0}\bar{D}^0$ threshold and the $D^0\bar{D}^0\pi^0$ energy distribution was peaked 2 to 3 MeV above the $D^{*0}\bar{D}^0$ threshold. This requires a negative value for $\mathrm{Re}\gamma$, which would correspond to a virtual state. They concluded that if the $D^0\bar{D}^0\pi^0$ threshold enhancement is associated with the $X(3872)$, then X must be a virtual state of charm mesons.

A crucial flaw in the analysis of Ref. [25] is that they assumed that the $D^0\bar{D}^0\pi^0$ contribution was proportional to $-\mathrm{Im}\,\kappa(E)$, where $\kappa(E) = (-2M_{*00}E - i\epsilon)^{1/2}$. This expression vanishes if $E < 0$. If the $X(3872)$ is a bound state with $\mathrm{Re}\gamma > 0$, most of the support of its line shape is in the region $E < 0$. Thus the assumption of Ref. [25] essentially forbids the bound state from decaying into $D^0\bar{D}^0\pi^0$. This is in direct contradiction to one of the universal features of an S-wave resonance near threshold. As the scattering length a increases to $+\infty$, the binding energy approaches $1/(M_{*00}a^2)$ and the mean separation of the constituents approaches $a/2$. In this limit, the decay of the resonance should be dominated by decays of its constituents. Since $D^0\pi^0$ is the largest decay mode of D^{*0}, $D^0\bar{D}^0\pi^0$ should be a dominant decay mode of the $X(3872)$ if it is a bound state. This flaw in the analysis of Ref. [25] could be removed by using the expression for $\kappa(E)$ in Eq. (20) to take into account the effects of the decays of the constituents of the $X(3872)$ resonance.

By comparing Eqs. (25) and (36), we can express the short-distance factor $\Gamma^{K^+}_{B^+}$ in terms of the parameters of Ref. [25]:

$$\Gamma^{K^+}_{B^+} = \frac{1}{\pi}(\mathcal{B}/g)\Gamma[B^+]. \tag{40}$$

The best fits in Ref. [25] give values of $\Gamma^{K^+}_{B^+}$ that range from 3.8×10^{-13} MeV to 4.9×10^{-13} MeV. This is one order of magnitude larger than the estimate for the short-distance factor in Eq. (34) with $\Lambda = m_\pi$. This requires the square of the matrix element $|\mathcal{M}|^2$ for $B^+ \to K^+ + D^{*0}\bar{D}^0$ near the $D^{*0}\bar{D}^0$ threshold to be larger than the average value $\langle|\mathcal{M}|^2\rangle$ defined by Eq. (30) not only by the threshold resonance factor $m_\pi^2|f(E)|^2$ but also by an additional order of magnitude.

VII. FITS TO THE ENERGY DISTRIBUTIONS

The line shapes of $X(3872)$ in the $J/\psi\pi^+\pi^-$ and $D^0\bar{D}^0\pi^0$ decay channels have been measured by the Belle and *BABAR* Collaborations for the production processes $B \to K + X$. In this section, we fit the Belle measurements for the production process $B^+ \to K^+ + X$ to a theoretical model for the line shapes that takes into account the width of the constituent D^{*0} as well as inelastic scattering channels for the charm mesons.

A. Experimental data

The Belle and *BABAR* Collaborations have both measured the energy distribution of $J/\psi\pi^+\pi^-$ near the $X(3872)$ resonance for the decay $B^+ \to K^+ + J/\psi\pi^+\pi^-$ [1,4]. The *BABAR* data has larger error bars, so we will consider only the Belle data. The Belle data on the $J/\psi\pi^+\pi^-$ energy distribution is given in Fig. 2b of Ref. [1]. The figure shows the number of events per 5 MeV bin as a function of $M_{J/\psi\pi^+\pi^-}$ from 3820 MeV to 3920 MeV. If we use the CLEO measurement of the D^0 mass and the PDG value for the $D^{*0} - D^0$ mass difference, this corresponds to E extending from -51.8 MeV to $+48.2$ MeV. In Ref. [25], Hanhart *et al.* used only the 8 bins extending from -21.8 MeV to $+18.2$ MeV. They subtracted the linear experimental background shown in Fig. 2b of Ref. [1] to get the 8 data points given in Table I. Our values for the energies at the centers of the bins differ

from those in Ref. [25] by -0.2 MeV, because they used the PDG values for the masses M_0 and M_{*0} instead of using the CLEO value for M_0 and the PDG value for $M_{*0} - M_0$. In our analysis, we have chosen to omit the first data point in Table I so that the data points are more symmetric about $E = 0$. We will use a theoretical model for the energy distribution that is essentially 0 at $E = -19.3$ MeV, so including this point would simply increase the χ^2 by a constant 0.57. The 7 data points used in our analysis are plotted in Fig. 5. Note that there are only two bins in which the data differs from 0 by significantly more than one error bar.

The Belle Collaboration has measured the energy distribution of $J/\psi\pi^+\pi^-$ near the $X(3872)$ resonance for the decay $B \to K + D^0\bar{D}^0\pi^0$ [8]. The $D^0\bar{D}^0\pi^0$ energy distribution is shown in Fig. 2a of Ref. [8]. The figure shows the events per 4.25 MeV bin as a function of $M_{D^0\bar{D}^0\pi^0} - 2M_{D^0} - M_{\pi^0}$ from 0 MeV to 76.5 MeV. This corresponds to E extending from -7.14 MeV to $+69.36$ MeV. In Fig. 2a of Ref. [8], the data for $B^+ \to K^+ + X$ and $B^0 \to K^0 + X$ are combined in the same plot. The energy distributions for B^+ decay and B^0 separately were presented at the ICHEP 2006 conference [28]. In Ref. [25], Hanhart *et al.* used only the data for $B^+ \to K^+ + X$ in 5 bins extending from -2.89 MeV to $+18.36$ MeV. They subtracted the combinatorial background to obtain the data points for those 5 bins. To account for the remaining experimental background, which is an increasing function of E, they added a background term to the theoretical expression for $d\Gamma/dE$ and determined its coefficient by fitting to the data. That background term is weakly constrained by the 5 data points. We have therefore chosen to subtract the total experimental background instead of only the combinatorial background. The resulting data points are given in Table II. Our values for the energies at the centers of the bins differ from those in Ref. [25] by -0.34, because they used the PDG values for the masses M_0 and M_{*0} to determine the $D^{*0}\bar{D}^0$ threshold instead of using the CLEO value for M_0 and the PDG value for $M_{*0} - M_0$. The first data point in Table II was omitted in the analysis of Ref. [25], because it would have given a constant contribution to χ^2 of 0.17. In our analysis, we have chosen to include this data point even though its effect on our analysis is negligible. The 6 data points used in our analysis are plotted in Fig. 6. Note that there is only one bin in which the data differs from 0 by significantly more than one error bar.

The analysis of Ref. [25] also used the Belle measurement of the branching ratio for decays of $X(3872)$ into $J/\psi\pi^+\pi^-\pi^0$ and $J/\psi\pi^+\pi^-$ [5]:

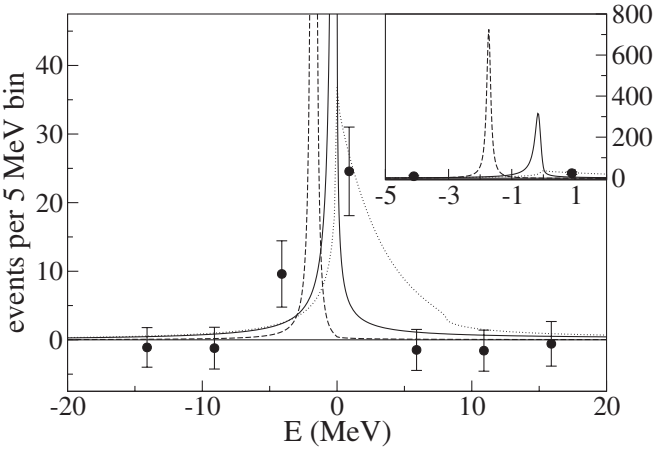

FIG. 5. Number of events per 5 MeV bin for $B^+ \to K^+ + J/\psi\pi^+\pi^-$ as a function of the total energy E of $J/\psi\pi^+\pi^-$ relative to the $D^{*0}\bar{D}^0$ threshold. The data points, which are given in Table I, were obtained by subtracting the linear experimental background from the data of the Belle Collaboration in Ref. [1]. The theoretical curves are the differential number distributions dN/dE in Eq. (43) multiplied by the 5 MeV bin width. The three curves correspond to the global minimum of χ^2 (dashed lines), the local minimum of χ^2 (solid lines), and the fit A_{Belle} of Ref. [25] (dotted lines). The inset shows the peaks of the distributions.

TABLE I. Belle data on the $J/\psi\pi^+\pi^-$ energy distribution: numbers of events N and their uncertainties ΔN in 5 MeV bins centered at the energies E. The numbers of events N were obtained from Fig. 2b of Ref. [1] by subtracting the linear experimental background. We used only the last 7 data points in our analysis.

E	N	ΔN
-19.3	-2.10	2.78
-14.3	-1.10	2.89
-9.3	-1.21	3.04
-4.3	9.60	4.83
0.7	24.56	6.46
5.7	-1.47	2.99
10.7	-1.57	2.99
15.7	-0.58	3.25
last 7 bins	28.23	10.54

TABLE II. Belle data on the $D^0\bar{D}^0\pi^0$ energy distribution: numbers of events N and their uncertainties ΔN in 4.25 MeV bins centered at the energies E. The numbers of events N were obtained from Ref. [28] by subtracting the total experimental background. Only the last 5 data points were used in the analysis of Ref. [25].

E	N	ΔN
-5.015	0.42	1.03
-0.765	0.90	1.38
3.485	11.58	4.13
7.735	1.35	2.82
11.985	1.50	3.30
16.235	-0.89	3.09
all 6 bins	14.86	6.96

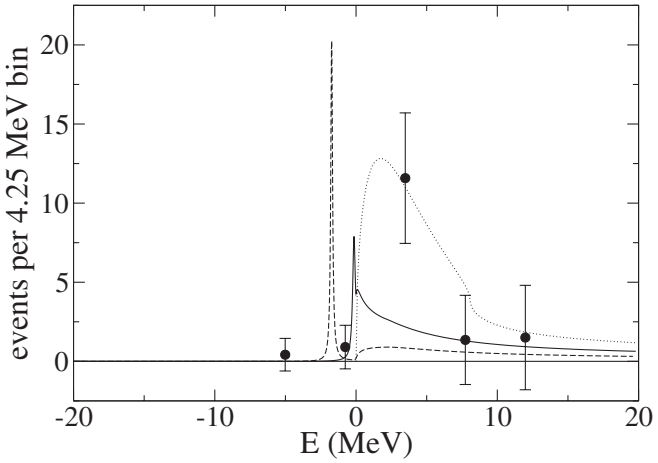

FIG. 6. Number of events per 4.25 MeV bin for $B^+ \to K^+ + D^0\bar{D}^0\pi^0$ as a function of the total energy E of $D^0\bar{D}^0\pi^0$ relative to the $D^{*0}\bar{D}^0$ threshold. The data points, which are given in Table II, were obtained by subtracting the total experimental background from the data of the Belle Collaboration in Ref. [8]. The theoretical curves are the differential number distributions dN/dE in Eq. (44) multiplied by the 4.25 MeV bin width. The three curves correspond to the global minimum of χ^2 (dashed line), the local minimum of χ^2 (solid line), and the fit $A_{\rm Belle}$ of Ref. [25] (dotted lines).

$$\frac{\mathrm{Br}[X \to J/\psi\pi^+\pi^-\pi^0]}{\mathrm{Br}[X \to J/\psi\pi^+\pi^-]} = 1.0 \pm 0.4 \pm 0.3. \qquad (41)$$

The signal region for $J/\psi\pi^+\pi^-\pi^0$ included only energies E within 16.5 MeV of 3872 MeV. Using the CLEO value for M_0 and the PDG value for $M_{*0} - M_0$, this corresponds to $-16.3\ \mathrm{MeV} < E < +16.7\ \mathrm{MeV}$.

B. Theoretical model

We summarize our model for the $X(3872)$ lines shapes in the channels $J/\psi\pi^+\pi^-$, $J/\psi\pi^+\pi^-\pi^0$, and $D^0\bar{D}^0\pi^0$ channels. The $J/\psi\pi^+\pi^-$ and $J/\psi\pi^+\pi^-\pi^0$ energy distributions are given by Eq. (26), while the $D^0\bar{D}^0\pi^0$ energy distribution is given in Eq. (27). The scattering amplitude $f(E)$ is given by Eq. (16) with $\mathrm{Im}\,\gamma$ replaced by $\Gamma^{J/\psi\pi^+\pi^-}(E) + \Gamma^{J/\psi\pi^+\pi^-\pi^0}(E)$:

$$f(E) = [-\mathrm{Re}\gamma - i\Gamma^{J/\psi\pi^+\pi^-}(E) - i\Gamma^{J/\psi\pi^+\pi^-\pi^0}(E) + \kappa(E)]^{-1}. \qquad (42)$$

The energy dependence of the functions $\Gamma^{J/\psi\pi^+\pi^-}(E)$ and $\Gamma^{J/\psi\pi^+\pi^-\pi^0}(E)$ are shown as solid lines in Fig. 2. Their normalizations are determined by $\Gamma_0^{\psi 2\pi} \equiv \Gamma^{J/\psi\pi^+\pi^-}(0)$ and $\Gamma_0^{\psi 3\pi} \equiv \Gamma^{J/\psi\pi^+\pi^-\pi^0}(0)$, which we treat as adjustable parameters. The function $\kappa(E)$ in Eq. (42) is given in Eq. (20). The functions $\Gamma_{*0}(E)$ and $\mathrm{Br}_{000}(E)$ are given in Eqs. (11) and (12), respectively. Thus our model has 4 adjustable real parameters: $\mathrm{Re}\gamma$, $\Gamma_{B^+}^{K^+}$, $\Gamma_0^{\psi 2\pi}$, and $\Gamma_0^{\psi 3\pi}$.

To translate the differential rates $d\Gamma/dE$ into numbers of events in the Belle experiment, we follow the prescription used in Ref. [25]. The differential number of $J/\psi\pi^+\pi^-$ events at the energy E is

$$\frac{dN}{dE}[J/\psi\pi^+\pi^-] = \frac{N_{\rm observed}^{J/\psi\pi^+\pi^-}\tau[B^+]/\hbar}{\mathrm{Br}[B^+ \to K^+ + X]\mathrm{Br}[X \to J/\psi\pi^+\pi^-]} \times \frac{d\Gamma}{dE}[B^+ \to K^+ + J/\psi\pi^+\pi^-]. \qquad (43)$$

For the number of observed events, we use the central value in Ref. [1]: $N_{\rm observed}^{J/\psi\pi^+\pi^-} = 35.7$. For the product of branching fractions in the denominator, we use the central value in Ref. [1], which is 1.3×10^{-5}. The differential number of $D^0\bar{D}^0\pi^0$ events at the energy E is

$$\frac{dN}{dE}[D^0\bar{D}^0\pi^0] = \frac{N_{\rm observed}^{D^0\bar{D}^0\pi^0}\tau[B^+]/\hbar}{\mathrm{Br}[B^+ \to K^+ + D^0\bar{D}^0\pi^0]} \times \frac{d\Gamma}{dE}[B^+ \to K^+ + D^0\bar{D}^0\pi^0]. \qquad (44)$$

For the number of observed events, we use the central value in Ref. [8]: $N_{\rm observed}^{D^0\bar{D}^0\pi^0} = 17.4$. For the branching fraction in the denominator, we use the central value in Ref. [8], which is 1.02×10^{-4}.

Following Ref. [25], we take into account the Belle measurement of the branching ratio in Eq. (41) through a constraint on the parameters of our theoretical model. We demand that

$$\frac{\Gamma[B^+ \to K^+ + J/\psi\pi^+\pi^-\pi^0; |E| < 16.5\ \mathrm{MeV}]}{\Gamma[B^+ \to K^+ + J/\psi\pi^+\pi^-; |E| < 16.5\ \mathrm{MeV}]} = 1.0. \qquad (45)$$

This constraint determines the ratio $\Gamma_0^{\psi 3\pi}/\Gamma_0^{\psi 2\pi}$ as a function of the parameters $\mathrm{Re}\,\gamma$ and $\Gamma_0^{\psi 2\pi}$. If we combine the errors in Eq. (41) in quadrature, the error bar on the right side of Eq. (45) is ± 0.5. We ignore this error bar and constrain the ratio in Eq. (45) to be 1.0 so that our results can be compared more directly with those in Ref. [25].[1]

C. Fitting procedure

One of the most important issues is whether the data on the $X(3872)$ is compatible with it being a bound state (corresponding to $\mathrm{Re}\,\gamma > 0$) or whether it must be a virtual state (corresponding to $\mathrm{Re}\,\gamma < 0$) as advocated in Ref. [25]. We therefore analyze the Belle data by fixing the parameter $\mathrm{Re}\,\gamma$ and minimizing the χ^2 with respect to the other 3 adjustable parameters $\Gamma_{B^+}^{K^+}$, $\Gamma_0^{\psi 2\pi}$, and $\Gamma_0^{\psi 3\pi}$ subject to the constraint in Eq. (45). The χ^2 is the sum of 13 terms corresponding to the last 7 data points in Table I and the 6 data points in Table II. The constraint in Eq. (45) determines the ratio $\Gamma_0^{\psi 3\pi}/\Gamma_0^{\psi 2\pi}$ for fixed $\mathrm{Re}\,\gamma$. In Fig. 7,

[1]In Ref. [25], the partial widths on the right side of Eq. (45) were integrated over the larger region $|E| < 20$ MeV, but this difference has a negligible effect on the analysis.

we show the minimum value of χ^2 with respect to variations of the two remaining parameters $\Gamma_{B^+}^{K^+}$ and $\Gamma_0^{\psi 2\pi}$ as a function of Re γ. The global minimum is $\chi^2 = 8.3$ at Re $\gamma = 57.8$ MeV. There is also a local minimum at Re $\gamma = 17.3$ MeV with $\chi^2 = 10.0$. Since Re $\gamma > 0$ for both the global minimum and the local minimum, these fits correspond to a bound state. For the sake of comparison, the $A_{\rm Belle}$ fit of Ref. [25] gives $\chi^2 = 19.1$. The real part of the inverse scattering length for this fit is Re $\gamma = -48.9$ MeV. Since this is negative, this fit corresponds to a virtual state. In Fig. 7, the value of χ^2 for the $A_{\rm Belle}$ fit is shown as a dot that lies just above the line.

In Table III, we list the parameters and the values of χ^2 for the global minimum, the local minimum, and the fit $A_{\rm Belle}$ of Ref. [25]. For the fit $A_{\rm Belle}$, Re γ is the real part of the inverse scattering length, $\Gamma_{B^+}^{K^+}$ is given in Eq. (40), and $\Gamma_0^{\psi 2\pi}$ and $\Gamma_0^{\psi 3\pi}$ are the values of $\Gamma_{\pi^+\pi^- J/\psi}(E)/g$ and $\Gamma_{\pi^+\pi^-\pi^0 J/\psi}(E)/g$ at $E = 0$. Our order-of-magnitude estimate for $\Gamma_{B^+}^{K^+}$ is given in Eq. (34) with $\Lambda = m_\pi$. The values of $\Gamma_{B^+}^{K^+}$ for the global minimum and the local minimum of χ^2 are more consistent with this estimate than the fit $A_{\rm Belle}$ of Ref. [25].

The line shapes of $X(3872)$ in the $J/\psi\pi^+\pi^-$ and $D^0\bar{D}^0\pi^0$ decay channels for various fits are shown together with the Belle data in Figs. 5 and 6, respectively. The line shapes corresponding to the local minimum, the global minimum, and the fit $A_{\rm Belle}$ of Ref. [25] are shown as solid, dashed, and dotted lines, respectively. The data points in these figures should be compared to the average values of the curves over the appropriate bins centered on the data points. The global minimum of χ^2 is somewhat pathological in that for both $J/\psi\pi^+\pi^-$ and $D^0\bar{D}^0\pi^0$ the integral of the line shape over a bin is largest not in the bin with the highest data point, but in the next lower bin. For the local minimum of χ^2, the integrated line shape gives a good fit to

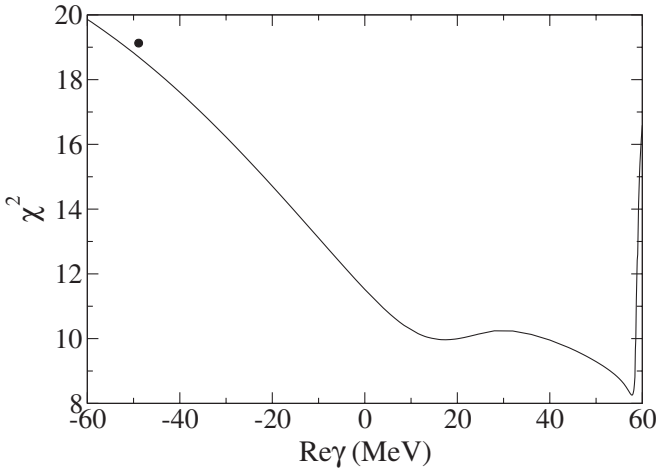

FIG. 7. The minimum χ^2 for the 13 data points in Figs. 5 and 6 as a function of Reγ. The χ^2 has been minimized with respect to the parameters $\Gamma_{B^+}^{K^+}$, $\Gamma_0^{\psi 2\pi}$, and $\Gamma_0^{\psi 3\pi}$ subject to the constraint in Eq. (45). The dot is the χ^2 for the fit $A_{\rm Belle}$ of Ref. [25].

TABLE III. Parameters (in units of MeV) and values of χ^2 for three fits to the subtracted Belle data: the global minimum of χ^2, the local minimum of χ^2, and the fit $A_{\rm Belle}$ of Ref. [25].

Fit	Reγ	$\Gamma_{B^+}^{K^+} \times 10^{14}$	$\Gamma_0^{\psi 2\pi}$	$\Gamma_0^{\psi 3\pi}$	χ^2
Global minimum	+57.8	4.1	0.44	0.50	8.3
Local minimum	+17.3	8.3	2.3	2.4	10.0
$A_{\rm Belle}$ of Ref. [25]	−48.9	38	0.93	0.71	19.1

the data point in the highest bin for $J/\psi\pi^+\pi^-$ but it is smaller than the data point in the highest bin for $D^0\bar{D}^0\pi^0$ by more than 2 standard deviations.

VIII. DISCUSSION

We have developed an approximation to the line shapes of the $X(3872)$ that takes into account the width of its constituents D^{*0} or $\bar{D}^{*0}$ as well as inelastic scattering channels for $D^{*0}\bar{D}^0$ and $D^0\bar{D}^{*0}$. The best combined fit to the Belle data on the energy distributions for the X resonance in the $J/\psi\pi^+\pi^-$ and $D^0\bar{D}^0\pi^0$ channels corresponds to a bound state with Re $\gamma > 0$, although a virtual state with Re $\gamma < 0$ is not excluded. Our results are in contradiction to the conclusions of Ref. [25]. By fitting essentially the same data, they concluded that the $X(3872)$ must be a virtual state. One flaw in their analysis was that they did not allow for decays of the constituent D^{*0} or $\bar{D}^{*0}$ in the case where the X is a bound state.

Our theoretical model for the line shapes is based on the assumption that the inverse scattering length in the $(D^*\bar{D})_+^0$ channel is small compared to all other relevant momentum scales. The line shapes are determined by the scattering amplitude $f(E)$ for charm mesons in the $(D^*\bar{D})_+^0$ channel given in Eq. (42). This amplitude contains no information about some of the other nearby thresholds, including the $D^{*+}D^-$ threshold at $E = +8.1$ MeV and the $D^0\bar{D}^0\pi^0$ threshold at $E = -7.1$ MeV. Thus the line shapes can be expected to be accurate only when $|E|$ is much less than 7 MeV. However the maxima of the line shapes are well within the region of validity. For the local minimum of χ^2, the peaks in the line shapes are near $E = -0.17$ MeV for $J/\psi\pi^+\pi^-$ and near $E = -0.14$ MeV for $D^0\bar{D}^0\pi^0$. For the global minimum of χ^2, the peaks in the line shapes are near $E = -1.7$ MeV for both $J/\psi\pi^+\pi^-$ and $D^0\bar{D}^0\pi^0$. The effects of the other thresholds would be dramatic only when $|E|$ is large enough that the line shapes are already small. They would be unlikely to change our qualitative conclusion that the best fit to the data corresponds to a bound state.

The range of validity of our model for the line shapes could be extended by taking into account explicitly scattering channels for the charged charm mesons $D^{*+}D^-$ and D^+D^{*-}. A first step in this direction has been taken by Voloshin [29]. He showed that the isospin symmetry breaking pattern of QCD provides interesting constraints on the line shapes. In particular, he predicted a zero in the line

shape of $X(3872)$ in the $J/\psi\pi^+\pi^-\pi^0$ channel between the $D^{*0}\bar{D}^0$ and $D^{*+}D^-$ thresholds. We have carried out a more rigorous two-channel analysis [30]. Given a plausible dynamical assumption, we find that the line shape of X in the $J/\psi\pi^+\pi^-\pi^0$ channel has a zero between the $D^{*0}\bar{D}^0$ and $D^{*+}D^-$ thresholds in the decays $B^+ \to K^+ + X$ but not in the decays $B^0 \to K^0 + X$. We also find that the line shape of X in the $J/\psi\pi^+\pi^-$ channel can have a zero below the $D^{*0}\bar{D}^0$ threshold in the decays $B^0 \to K^0 + X$.

The accuracy of our predictions for the line shapes could be further improved by taking into account pions explicitly. The system consisting of $D^{*0}\bar{D}^0$, $D^0\bar{D}^{*0}$, and $D^0\bar{D}^0\pi^0$ states with energies near the $D^0\bar{D}^{*0}$ threshold can be described by a nonrelativistic effective field theory. The simplest such theory has S-wave scattering in the $(D^*\bar{D})^0_+$ channel and π^0 couplings that allow the decay $D^{*0} \to D^0\pi^0$. Fleming, Kusunoki, Mehen, and van Kolck developed power-counting rules for this effective field theory and showed that the pion couplings can be treated perturbatively [31]. They used the effective field theory to calculate the decay rate for $X(3872) \to D^0\bar{D}^0\pi^0$ to next-to-leading order in the pion coupling.

In applying this effective field theory to the line shapes of the $X(3872)$, one complication that will be encountered is infrared singularities at the $D^{*0}\bar{D}^0$ threshold that are related to the decay $D^{*0} \to D^0\pi^0$. This problem has been analyzed in a simpler model with spin-0 particles and momentum-independent interactions [32]. The problem was solved by a resummation of perturbation theory that takes into account the perturbative shift of the $D^0\bar{D}^{*0}$ threshold into the complex energy plane because of the nonzero width of the D^{*0}.

In summary, the establishment of the quantum numbers of the $X(3872)$ as 1^{++} and the measurement of its mass imply that it is either a charm meson molecule or a charm meson virtual state. The existing data favor a charm meson molecule, but a virtual state is not excluded. To decide conclusively between these two possibilities will require more extensive data on the line shapes of the $X(3872)$ in various decay channels and for various production processes.

ACKNOWLEDGMENTS

This research was supported in part by the Department of Energy under Grant No. DE-FG02-91-ER40690. We thank the authors of Ref. [25] for sharing with us the data points used in their analysis.

[1] S. K. Choi *et al.* (Belle Collaboration), Phys. Rev. Lett. **91**, 262001 (2003).
[2] D. Acosta *et al.* (CDF II Collaboration), Phys. Rev. Lett. **93**, 072001 (2004).
[3] V. M. Abazov *et al.* (D0 Collaboration), Phys. Rev. Lett. **93**, 162002 (2004).
[4] B. Aubert *et al.* (*BABAR* Collaboration), Phys. Rev. D **71**, 071103 (2005).
[5] K. Abe *et al.* (Belle Collaboration), arXiv:hep-ex/0505037.
[6] K. Abe *et al.* (Belle Collaboration), arXiv:hep-ex/0505038.
[7] A. Abulencia *et al.* (CDF Collaboration), Phys. Rev. Lett. **96**, 102002 (2006).
[8] G. Gokhroo *et al.* (Belle Collaboration), Phys. Rev. Lett. **97**, 162002 (2006).
[9] W. M. Yao *et al.* (Particle Data Group), J. Phys. G **33**, 1 (2006).
[10] C. Cawlfield *et al.* (CLEO Collaboration), Phys. Rev. Lett. **98**, 092002 (2007).
[11] N. A. Tornqvist, Phys. Lett. B **590**, 209 (2004).
[12] F. E. Close and P. R. Page, Phys. Lett. B **578**, 119 (2004).
[13] S. Pakvasa and M. Suzuki, Phys. Lett. B **579**, 67 (2004).
[14] M. B. Voloshin, Phys. Lett. B **579**, 316 (2004).
[15] E. Braaten and M. Kusunoki, Phys. Rev. D **69**, 074005 (2004).
[16] E. Braaten and H. W. Hammer, Phys. Rep. **428**, 259 (2006).
[17] E. Braaten, M. Kusunoki, and S. Nussinov, Phys. Rev. Lett. **93**, 162001 (2004).
[18] E. Braaten and M. Kusunoki, Phys. Rev. D **71**, 074005 (2005).
[19] E. Braaten and M. Kusunoki, Phys. Rev. D **72**, 014012 (2005).
[20] E. Braaten and M. Kusunoki, Phys. Rev. D **72**, 054022 (2005).
[21] E. Braaten and M. Lu, Phys. Rev. D **74**, 054020 (2006).
[22] E. S. Swanson, Phys. Rep. **429**, 243 (2006).
[23] L. Maiani, A. D. Polosa, and V. Riquer, arXiv:0707.3354 [Phys. Rev. Lett. (to be published)].
[24] D. V. Bugg, Phys. Lett. B **598**, 8 (2004).
[25] C. Hanhart, Yu. S. Kalashnikova, A. E. Kudryavtsev, and A. V. Nefediev, Phys. Rev. D **76**, 034007 (2007).
[26] B. Aubert *et al.* (*BABAR* Collaboration), Phys. Rev. D **68**, 092001 (2003).
[27] B. Aubert *et al.* (*BABAR* Collaboration), Phys. Rev. D **73**, 011101 (2006).
[28] G. Majumder, ICHEP2006 http://belle.kek.jp/belle/talks/ICHEP2006/Majumder.ppt.
[29] M. B. Voloshin, Phys. Rev. D **76**, 014007 (2007).
[30] E. Braaten and M. Lu (unpublished).
[31] S. Fleming, M. Kusunoki, T. Mehen, and U. van Kolck, Phys. Rev. D **76**, 034006 (2007).
[32] E. Braaten, M. Lu, and J. Lee, Phys. Rev. D **76**, 054010 (2007).